Sub-6 GHz Quad-Band Reconfigurable Antenna for 5G Cognitive Radio Applications

Sivakumar Ellusamy [1] and Ramachandran Balasubramanian [2]

[1] Department of Electronics and Communication Engineering
SRM Institute of Science and Technology, Chennai, Tamilnadu 603203, India
sivakume@srmist.edu.in

[2] Department of Electronics and Communication Engineering
SRM Institute of Science and Technology, Chennai, Tamilnadu 603203, India
ramachab@srmist.edu.in

Abstract ─ This article describes a quad-band frequency tunable antenna for 5G applications that operates in the sub-6 GHz frequency range. On the top side, a stub-loaded square patch is printed on an inexpensive glass epoxy substrate, and on the opposite side, a C-shaped slot embedded into the partial ground plane. To achieve frequency reconfigurability with a consistent radiation pattern, the C-shaped slot and matching stub are used. The antenna is electronically frequency tunable by placing two positive intrinsic negative diodes (PIN) in the C-shaped slot and one PIN diode between the stub and feed line. The frequency is tunable between one ultra-wideband (UWB) and three communication bands based on the switching conditions of the PIN diodes. The proposed configuration is small, with a substrate dimension of $25 \times 25 \times 1$ mm^3. The antenna was fabricated, tested and found measurements result back up the simulation; it can switch between UWB (3.31.0-6.03 GHz) and three communication modes (3.31-4.32, 3.78-4.98, 4.98-5.96 GHz). The antenna has peak gains of 1.91, 1.86, 2.0 and 2.0 dB, and radiation efficiencies of 80, 78, 83 and 86%, respectively, in the four frequency bands. The developed antenna is ideally suited for multi-functional wireless systems and cognitive radio applications since it covers the frequency bands below 6 GHz and is tunable between wide and narrow bands.

Index Terms ─ Narrow band, PIN diode, quad-band, reconfigurable, square patch, stub, tunable, ultra wide band.

I. INTRODUCTION

Implementation of the future communication system (5G) is probably either in sub-6GHz or in the mm-wave region. The research in 5G is growing since the demand for high data rates and better performance are ever-increasing. Coverage, adequate signal quality, low latency, and so on, are just a few of the benefits sparked interest in 5G networks [1,2]. The 5G spectrum are divided into three operating region. They are below 1 GHz (Low-Bands), between 1-6 GHz (Mid-Bands), and above 24 GHz (mm-wave). For 5G deployment, several countries are mainly concentrating on the mid-band (3-6GHz) and mm-wave (24 GHz). Higher frequencies have higher propagation losses, so the mid-band frequency was chosen over the mm-wave frequency [3]. Nowadays, wireless systems are becoming more multifunctional, necessitating the use of mobile devices that operate on various standards or applications. Reconfigurable antennas are advanced antenna that can adjust its resonant frequency, impedance bandwidth, radiation pattern, and polarization to achieve multi-functionality. The reconfigurable antenna is a single element that supports multiple wireless standards in a single unit, as opposed to traditional antennas. However, more conventional antennas are required to maintain the various wireless standards [4].

Multiple-input-multiple-output (MIMO), cognitive radio (CR), and beamforming technologies are all essential in the implementation of 5G systems. The cognitive radio is a cutting-edge technology that improves spectrum efficiency in modern communication systems. Furthermore, the cognitive radio requires a wideband antenna for scanning the whitespace within the finite frequency spectrum of interest. A reconfigurable communicating antenna to transmit/receive the information in the unoccupied frequency bands [5]. For the past few years, antenna design for CR has been a hot research subject. The researchers are interested in developing frequency tunable antennas as well as a sensing antenna. The authors of [6] discussed cognitive radio architecture, working process, as well as possible antenna configurations and design approaches. Cognitive radio are drawn to frequency reconfigurable antennas because they can dynamically change their resonant frequency to meet device requirements. They have various features

such as efficient utilization of spectrum, compact size, easy integration, operation in wide and narrowbands, and frequency selectivity characteristics to avoid co-site interference. Electrical, mechanical, material change, and optical techniques can all be used to achieve reconfigurability in an antenna. Electrical and electro-mechanical devices such as varactor diodes [7], PIN diodes [8-11], and RF MEMS are the most widely used reconfiguration techniques [12].

Several prototypes for CR applications are available in the literature [13-17]. A wide-band antenna and slot radiator were used in the design mentioned in [13]. The UWB antenna operates between 3 and 11 GHz, while a slot-radiator serves as a reconfigurable communicating antenna between 5 and 6 GHz. The mechanical rotation is used in the antenna structure in [14] to achieve frequency tunability. A wide-band antenna for monitoring the spectrum between 2 and 6 GHz and a communicating antenna for data transmission/reception within the UWB band were reported in another design in [15]. In this configuration, the height and angle of the ground plane are changed for frequency tuning. A compound tunable antenna with sensing capability was reported in [16], and it was able to detect the band from 3 to 12 GHz and communicate in five narrowbands from 1.73 to 5.23 GHz. For cognitive radio applications, [17] describes a multi-port antenna system. The antenna has four narrowband communication modes and can sense between 3.1 to 10.6 GHz. Separate antennas for sensing the channel and transmission/reception of data within the unoccupied channel are used in the literature [13-17]. These designs have complex structures, large physical size, and occupies more space. As a consequence, for cognitive radio applications, a single antenna with both sensing and communicating capabilities is highly desirable.

For CR applications, the designs reported in [18-23] use a single antenna capable of switching between wideband and narrowband. For reconfigurability, the proposed antenna in [18] uses filtering structures in the ground plane. In UWB mode, the antenna had a sensing range of 3.1 to 10.6 GHz and in narrowband mode, it covered five switchable states. The paper [19] introduced a frequency reconfigurable antenna with an integrated reconfigurable filter for CR application. The antenna can detect the spectrum from 2.63 to 3.7 GHz and function in four sub-bands. The reconfigurable antenna mentioned in the article [20] incorporates sensing and communication functionality. In sensing mode, the antenna covered 2.8-11.4 GHz and nearly covered three communication bands in the entire UWB spectrum for cognitive radio applications. A wideband radiator and a multifunctional tunable filter are included in the design in [21]. The antenna in this proposed design has all-pass, bandpass, and bandstop characteristics in the frequency range 2.5-4.2 GHz. For the sub-6 GHz band (2.5-4.2GHz), a single antenna system incorporating both MIMO and CR technologies has been reported [22]. It has sensing frequency range of 2.0-5.7GHz, with a bandpass response of 3.2-4.0GHz, and a band-notch response of 3.37-4.0GHz. The design [23] included a frequency reconfigurable MIMO mode as well as UWB MIMO mode. For reconfigurability, this design uses PIN and varactor diode. The antenna has broad sensing capability in the sensing band, ranging from 1 to 4.5 GHz, and continuous frequency tunability in the communication band, ranging from 0.9-2.6 GHz.

In the literature [13-17], two different antennas were used to provide sensing and communication functionality, resulting in increased physical size, increased space requirements, and complex structures. The designs in [18,21-23] use a single antenna for sensing and communication, but they do not cover the nR79 (4.4-5.0GHz) and sub-6 GHz range above 4.8-6.0 GHz. This paper describes a sub-6 GHz antenna system for cognitive radio. A square patch monopole antenna, slotted ground plane, and PIN diodes are included in the structure for frequency reconfigurability. In this structure, diodes are located in the ground plane and do not require vias and biasing lines for activation. The presented antenna has two modes: wideband mode and communication mode. The unique features and contribution of the proposed antenna are:

1) A single antenna performs both sensing and communication operation, so port isolation is not necessary.
2) Wide band sensing from 3.31 to 6.03 GHz, with data transmission/reception in three bands in communication mode, covering the bands 3.31-4.32, 3.78-4.98, 4.98-5.96 GHz.
3) A multifunctional filter is used to achieve sensing and communication functionality through a single antenna system.
4) Compact size of $25\times25\times1mm^3$ reduces the space requirement for CR applications.

The design aspects, parametric analyis and optimization is discussed in the Section II. Section III presents the simulated and experimental outcomes. Section IV is devoted to the conclusion.

II. METHODOLOGY

This section covers the basic antenna configuration as well as the evolution stages of quad-band frequency tunable antennas. The electromagnetic solver (HFSS) is used to model the proposed antenna. A lumped model of the diode is used as a switching device in the simulation environment to obtain frequency reconfigurability. The design has been optimized to get good impedance characteristics and far-field patterns.

A. Antenna geometry

Figure 1 presents the basic antenna configuration. It is etched on the top surface of FR-4 substrate with a thickness of 1mm, a relative permittivity of 4.4, and a dissipation factor of 0.02. The substrate has a total volume of $25 \times 25 \times 1 mm^3$. The microstrip feed line is simple and offers a planar structure. Therefore, the microstrip feed line is chosen to excite the radiator. A switchable C-shaped slot on the ground plane and a reconfigurable stub attached to the feed are used to make the antenna frequency reconfigurable. The slot length and shape determine the desired operating band and bandwidth.
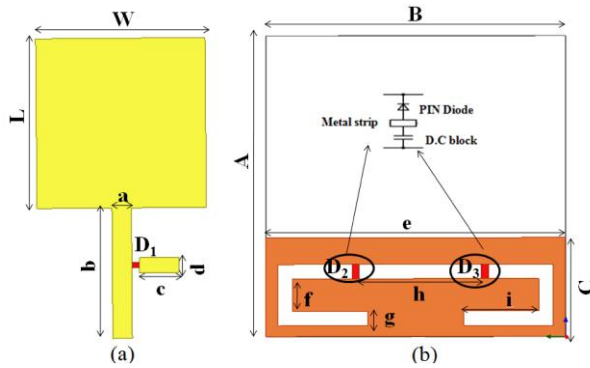

Fig. 1. The basic geometry: (a) top side and (b) back side.

B. Design and analysis

Figures 2 and 3 depict the narrow and wideband antenna design stages and their corresponding frequency responses. At first, the conventional square patch monopole UWB radiator is created, and the radiator length has selected to produce a lower resonance of 3.3 GHz using the following design equation [24,25].

The lower resonance f_L is calculated by:

$$f_L = \frac{7.2}{L+r+p} GHz .$$ (1)

The L and r are estimated as follows for the square-shaped monopole radiator. If W is the width of radiator, then,

$$L = W , \quad r = \frac{W}{2\pi} ,$$ (2)

and p is the distance between the monopole radiator and the ground plane.

Figure 2 depicts the frequency response of the UWB radiator without a slot, which has an impedance bandwidth ($S_{11} < -10$ dB) of 3.3-6.57 GHz.
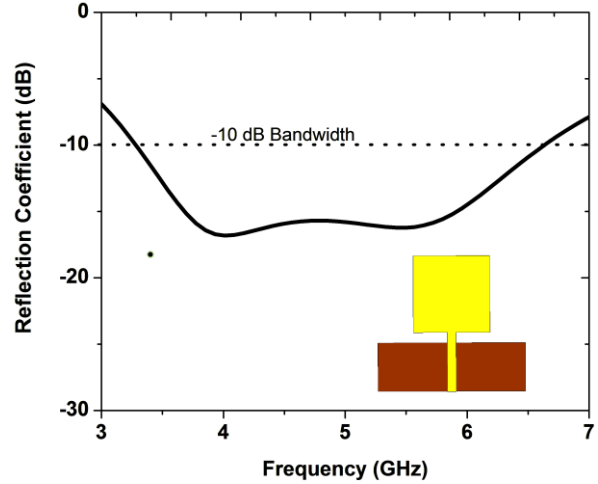

Fig. 2. UWB antenna and reflection coefficient.

Next, a horizontal slot is placed on the ground plane of the UWB radiator. The embedded slot below the feed line function as a bandstop filter that attenuates the desired frequency band (3.3-6.57 GHz) and leaves a passband between them [Antenna 1]. The effective length of the horizontal slot is determined using the following relation given in [24]:

$$L_{slot} = \frac{c}{2 f_r \sqrt{\varepsilon_e}} ,$$ (3)

where f_r is the lower resonance, c is the velocity of light and ε_e is an effective dielectric constant of the substrate material. The width of the stopband is controlled by the width of the slot. It has been set to 1.2mm, which is approximately the physical dimension of the PIN diode. The next step is shortening the horizontal slot length in Antenna 1 [Antenna 2], which results in a narrow passband of 3.85-4.86 GHz, but the matching is poor. The rectangular stub is added, provides additional reactive loading, and dramatically improves the feed line and radiator matching. Hence, Antenna 2 has strong matching and passband characteristics of 3.85-4.86 GHz. Following that, the introduction of a U-shaped slot in Antenna 2 without stub [Antenna 3] resulted in bandpass characteristics of 4.86-5.87 GHz. Antenna 3 was then changed by inserting another U-shaped slot, resulting in Antenna 4, which has a higher bandwidth due to additional capacitive effects. As a result, Antenna 4 acts as a UWB radiator with a bandwidth of 3.38-5.96 GHz. The proposed antenna is then constructed by combining narrowband (Antenna 2) and wideband (Antenna 4) antennas. It has bandpass response from 3.38-4.24GHz.

(a) Evaluation of narrow and wideband antenna
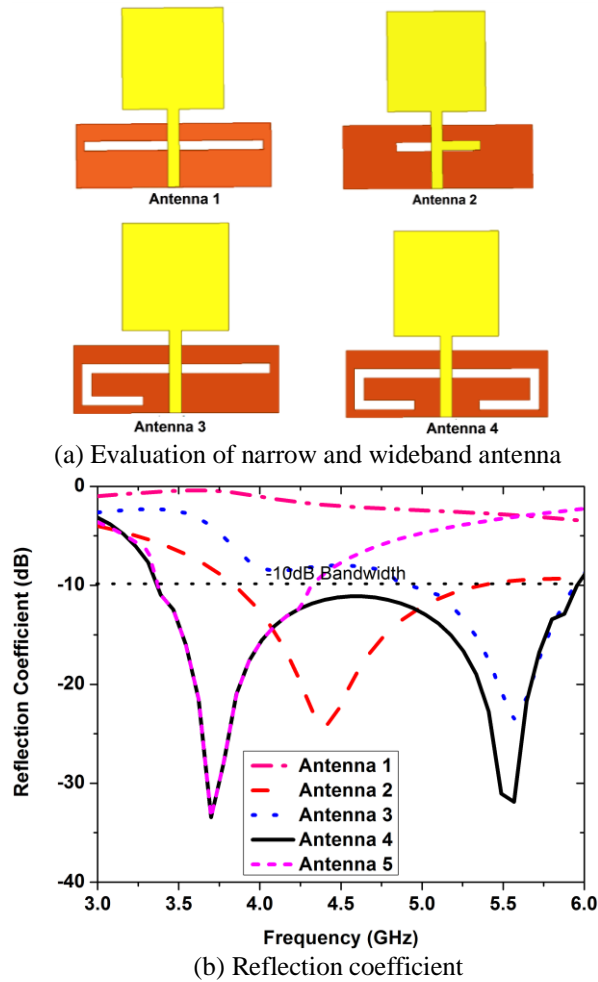

(b) Reflection coefficient

Fig. 3. Various design structures and their corresponding reflection coefficient.

The evolution of the proposed design providing capability of narrow and wideband responses is shown in Fig. 4. The combination of the horizontal slot, two U-shaped slots, and rectangular stub forms the multi-purpose filter, controlling the frequency between narrow and wideband responses.

Fig. 4. Evolution of the proposed antenna.

The parametric investigation is conducted to understand the functioning of the antenna, i.e., in Antenna 2 and Antenna 4, and to avoid measurement errors. There are over 12 design variables to study. The height of the ground (C), length (e,f, i) and width of the C-shaped slot (g) and stub (c and d), have a significant influence on frequency response.

The S-parameter curves in Fig. 5 (a) visualize the changes in reflection coefficient (S_{11} in dB) as the height of the ground plane in Antenna 4 is varied while all other parameters remain constant. The gap between the radiator and the ground plane changes as the height grows from 7.8mm to 8.4mm, causing the bandwidth to shift. When C is 8.2mm, and all other parameters are held constant, a good characteristic for S_{11} and bandwidth is obtained. Fig. 5 (b) indicates the effect in reflection coefficient for various lengths of the long horizontal slot. The graph illustrates that shortening the slot decreases antenna bandwidth while also affecting matching. The value of e=23mm was found to be the optimum compromise for improved reflection coefficient and bandwidth. The impact of changing the length of the vertical slot (f), the small horizontal slot (i), and the slot width (g) is shown in Figs. 5 (c)-(e). The antenna loses matching at the mid-frequency region as the vertical slot length decreases. Similarly, changing the length of the horizontal slot has the same effect. The antenna has an excellent S_{11} and bandwidth for parameter values of e=23mm, f=2.7mm, i=6.3mm, and g=1.2mm.

The impact of the rectangular stub on antenna performance has also been studied in Antenna 2. Figure 5 (d) depicts the reflection coefficient of the antenna for various stub lengths. When the stub length is trimmed from 5mm to 1mm, the antenna deviates significantly from the target application band, and antenna impedance matching is particularly poor for small length.The value of c equal to 4.5mm yields the best simulation results for S_{11} characteristics and bandwidth. The stub width was also varied to test the antenna's performance, as illustrated in Fig. 5 (e). As the width drops from 1.5mm to 0.8mm, the reflection coefficient declines from its maximum value, causing the antenna to deviate significantly from the desired application band. The values of d equal to 1mm, 1.1mm, and 1.2mm deliver the best simulation results. However, d equal to 1.2mm produces the best results not only in Antenna 2 but also in Antenna 5. The proposed antenna,according to the study, has the best frequency response for the optimized parameters, which are as follows: A = 25mm, B = 25mm, C = 8.2mm, L = 13mm, W = 13mm, a = 1.5mm, b = 10mm, c = 4.4mm, d = 1.2mm, e = 23mm, f = 2.7mm, g = 1.2mm, h = 12.2mm, and i = 6.3mm.
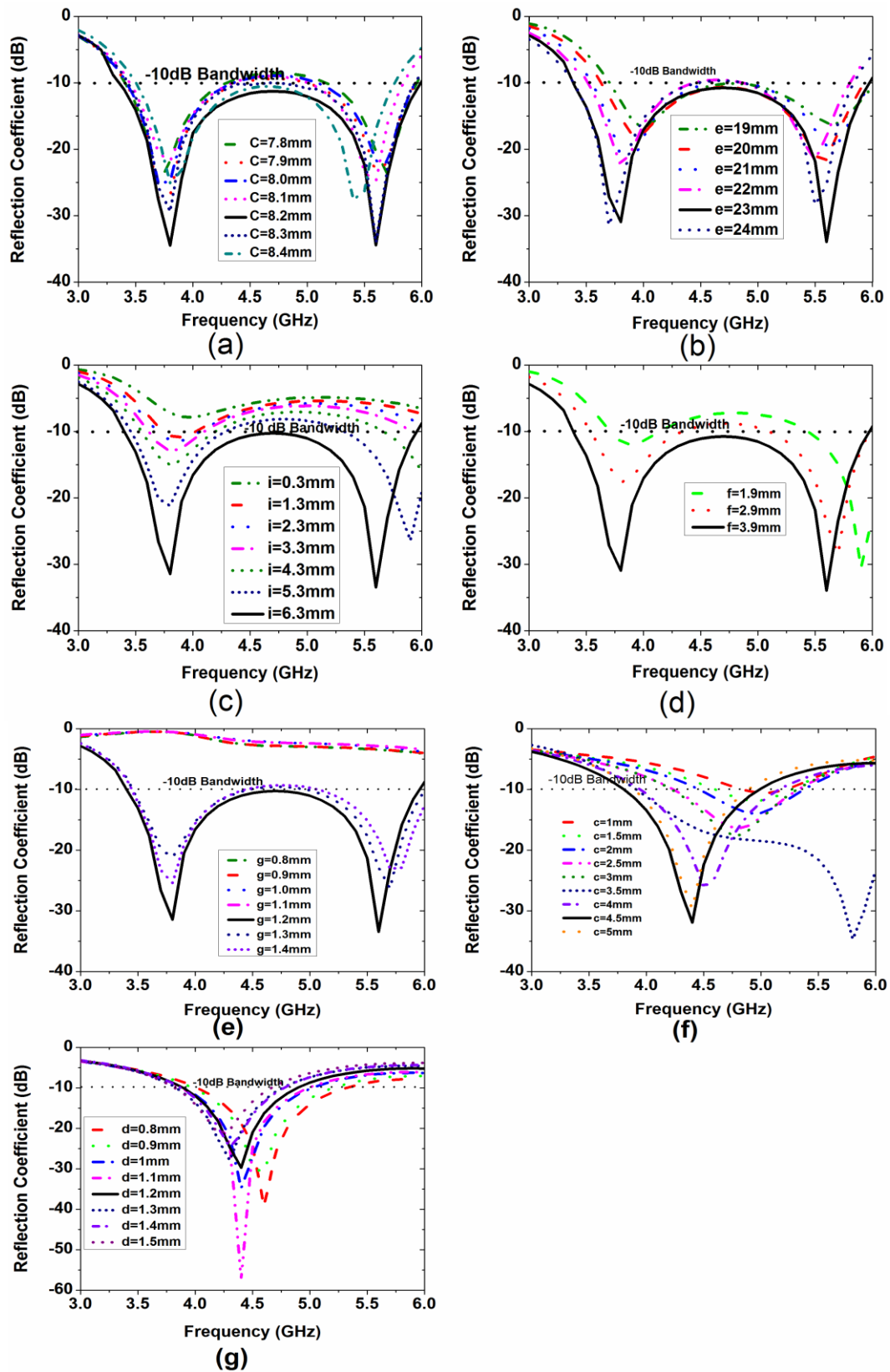
Fig. 5. Simulated reflection coefficients for (a) variations in ground plane height, (b)-(e) variations in slot parameters, and (f)-(g) variations in stub parameters.

C. Optimization

After the parametric study is performed, the genetic algorithm is used for further optimization. The height of the ground (C), length (e,f, i) and width of the C-shaped slot (g) and stub (c and d) is chosen to be the optimized parameters. Based on the optimetric study, the minimum and maximum values are taken for each parameters are 50% and 150% of the nominal values of initial design. The reflection coefficient is defined as cost function ($\leq$-10dB) in the frequency range (3-6GHz) for Antenna 4 and (3.8-5.3GHz) for Antenna 2.

In the GA optimizer, the following setup is kept for the optimization process, maximum number of generations is 200, number of parents are 30, number of mating pools is 30, number of children is 30, number of survivors is 10, and selection pressure for next generation is 10. A uniform distribution mutation type is used in the reproduction setup with 0.1 uniform mutation probability, 0.5 individual mutation probability, 0.2 variable mutation probability, and 0.05 standard deviation [26]. The optimized values of the parameters are presented in Table 1.

Table 1: Initial and optimized values obtained from the genetic algorithm

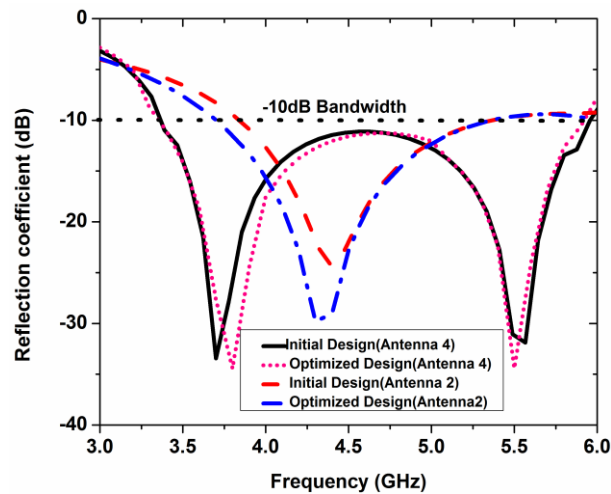|	Antenna 2			Antenna 4	
Parameters	**Initial Design Values (mm)**	**Optimized Values (mm)**	**Parameters**	**Initial Design Values (mm)**	**Optimized Values (mm)**
C	8.2	8.25	C	8.2	8.27
c	4.4	4.47	c	23	23
d	1.2	1.17	d	2.7	2.7
e	12.2	12.26	e	6.3	6.3
g	12	1.19	g	1.2	1.2

Fig. 6. Reflection coefficient curves for initial and optimized design.

Figure 6 depicts the reflection coefficient findings for the initial and optimized designs. It can be observed that the optimized Antenna 2 has a better bandwidth than the original design and a low reflection coefficient. However, in Antenna 4, a minor shift in bandwidth and reflection coefficient is seen.

D. Reconfigurable antenna

A quad-band reconfigurable antenna is designed by controlling the slot length and connecting/disconnecting the stub to the feed line using Antenna 5 [proposed design] in Fig. 4. To obtain multi-mode characteristics, two switches D_2 and D_3 are connected in the slots, and D_1 is attached between the feed line and the stub (Proposed deisgn in Fig. 1). The various structures [Antenna 1-5] depicted in Fig. 3 are determined by the placement of the switches D_2 and D_3 in the slot at the appropriate positions. This design uses RF PIN diodes as switching element. Figures 7 (a)-(c) depicts the analogous lumped RLC boundary conditionof the PIN diode describing the ON and OFF states. In the ON condition, the diode has an ohmic resistance (R_s) of 2.1Ω and an inductance (L_s) of 0.6nH. In the OFF state, it has a series inductance (L_s) of 0.6nH and is connected to a parallel combination of resistance (R_p) and capacitance (C_t) of 3 KΩ and 0.17pF. However, since the lumped model provides short and open circuit action in the ON and OFF states, we did not consider the inductance and capacitance values in simulation. As a result, in simulation, the RF PIN diode is merely represented as lumped resistor. In the ON state, a lumped model with low resistance (2.1 Ω) exhibits short circuit behavior, allowing current to flow on the antenna structure. The lumped model with high resistance (3 KΩ), on the other hand, exhibits an open circuit behavior in the OFF state, preventing current flow in the antenna structure.

Figure 8 depicts the simulated frequency response of the proposed frequency-reconfigurable antenna. The antenna works in four different operating bands depending upon the configuration of the switches. If all of the switches are OFF, the antenna works in UWB mode; otherwise, it works in communication mode. In-state 1 (all diodes are ON), the antenna works at a single narrowband with an impedance bandwidth of

3.85-5.32 GHz. The antenna also operates at a single narrowband in state 2 (D1 ON, D2 OFF, D3 OFF) and state 3 (D1 OFF, D2 ON, D3 OFF). It has an impedance bandwidth of 3.38-4.24 GHz and 4.86-5.87 GHz, respectively. Finally, in state 4 (all diodes are OFF), the antenna works at a wideband covering 3.38-5.96 GHz.
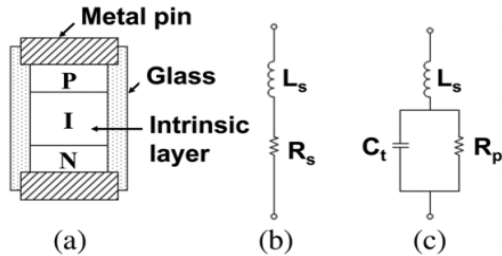

Fig. 7. PIN diode and its lumped model: (a) cross-section of diode, (b) forward bias, and (c) reverse bias.
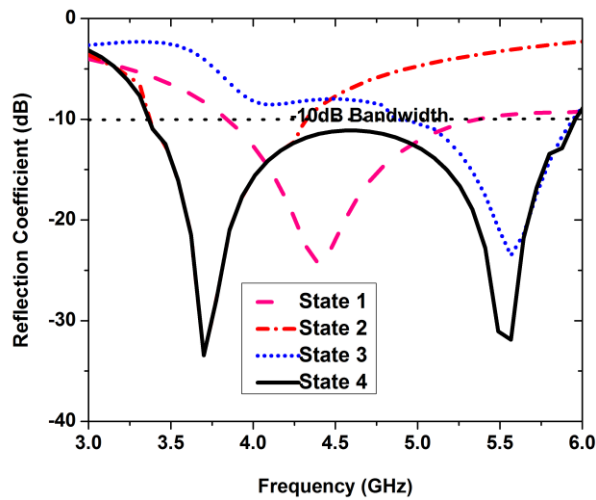

Fig. 8. Simulated reflection coefficient for different operating states.

Figure 9 depicts the surface current distribution in the slot for different switching states in order to better understand multi-band operation. The maximum current distribution aids in determining the slot length/part that contributes to each frequency band. Figure 9 (a) shows the maximum current density in state 1 at the middle of the slot and rectangular stub, As a consequence, the antenna opreates at 4.3 GHz, which covers the operating frequency range of 3.85 to 5.32 GHz.

The physical length of the slot, or the effective electrical length of the current distribution along the slot, is determined to be 0.25 λg, which corresponds to the resonant frequency 4.3 GHz. Where λg is the guide wavelength. Figures 9 (b)-(c) depicts the current distribution for states 2 and 3. In state 2, as visualized

in Fig. 9 (b), the current is distributed throughout the slot and dominates in the rectangular stub. The antenna resonates at 3.7 GHz covers the frequency band 3.38-4.24 GHz with electrical slot lengths of 1.13 λg. In state 3, however, the current distribution only dominates in half of the total slot length, as seen in Fig. 9 (c). As a result, the antenna resonates at 5.5 GHz with a slot length of 0.5λg, covering the frequency range of 4.86-5.87 GHz. Figures 9 (d)-(e) shows the current prevalent maximum across the entire slot and feed line, with no distribution in the rectangular stub. With a slot length of 1.13 λg, the antenna resonates at 3.7 and 5.5 GHz, covering the frequency range of 3.38-5.98 GHz. According to the analysis, a variation in the electrical length of the current distribution causes frequency reconfiguration/multiband operation in the antenna structure.
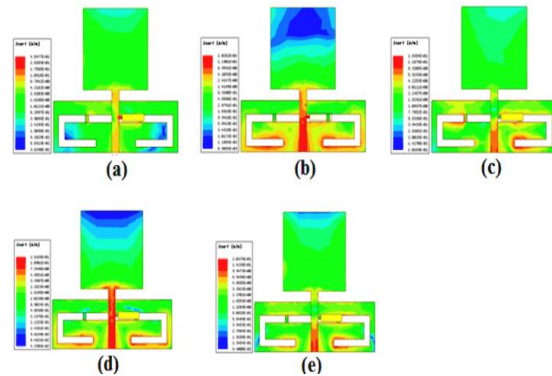

Fig. 9. The surface current distribution in various operational conditions: (a) state1 at 4.3 GHz, (b) state 2 at 3.7 GHz, (c) state 3 at 5.5 GHz, and (d)-(e) state 4 at 3.7 and 5.5 GHz.
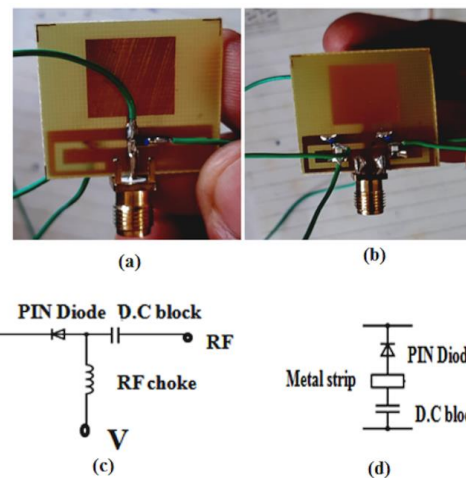

Fig. 10. Prototype and biasing structure (a) top side, (b) bottom side, (c) biasing circuit, and (d) biasing structure.

Table 2: Various operating states and their corresponding frequency band

Diodes	D1	D2	D3	Mode	Freq. Bands (GHz) Simulated/Measured
State 1	ON	ON	ON	Communication	3.85-5.32 / 3.78-4.98
State 2	ON	OFF	OFF	Communication	3.38-4.24 / 3.31-4.32
State 3	OFF	ON	ON	Communication	4.86-5.87 / 4.98-5.96
State 4	OFF	OFF	OFF	Sensing	3.38-5.96 / 3.31-6.03

III. FABRICATION AND RESULTS

The antenna is simulated and modeled using EM solver-High frequency structure simulator. Figures 10 (a)-(d) illustrates the antenna prototype with biasing circuits. After placing the PIN diodes in the proper locations, the proposed antenna is tested, and measured. The antenna is powered by a 50Ω SMA connector, and the frequency is tuned by controlling the slot length with an Infineon BAR 64-02 diode. The antenna structure has been modified to realize the proposed design with real diodes, as shown in Fig. 10 (d). A metal strip measuring 2.0×0.6 mm^2 is inserted into the slot to supply a dc voltage to the PIN diodes D_2 and D_3. A 100pF dc blocking capacitor is attached to the ground plane to provide an RF link to the diode while retaining dc isolation from the RF signal. To bias the diode, a battery applies a 1.5 V dc voltage to the metal strip. The d.c supply is directly given to diode D_1. The matching stub serves as an RF choke, preventing RF signals from entering the d.c supply.
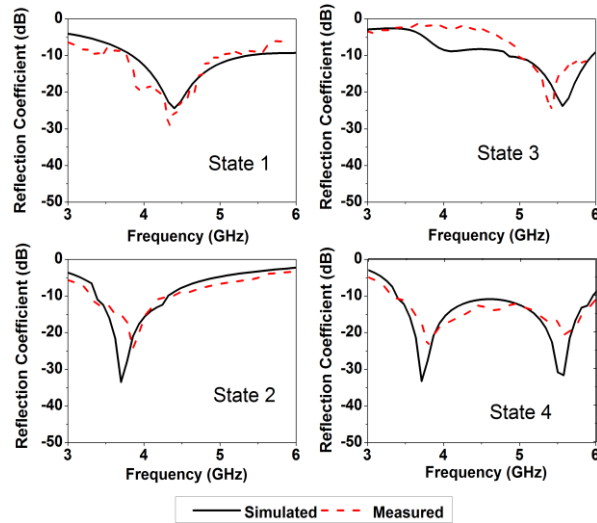

Fig. 11. Reflection coefficient for different operating states.

A. Reflection coefficient

The frequency response of the presented antenna is determined using a vector network analyzer. Figure 11 shows the input response of the presented design in simulation and measurements for various operating conditions of the diode. The designed antenna works in either the ultra wide-band or one of the three communication modes, based on the biasing conditions of the diodes. Table 2 summarizes the antenna switching conditions and their operating modes. In states 1, 2, and 3, the proposed antenna has narrow passband characteristics, while state 4 has wide-band characteristics. The simulated impedance bandwidth in state 1 is 3.85-5.32 GHz, while the measured value is 3.78-4.98 GHz. The antenna impedance bandwidth is 3.38-4.24 GHz in simulation, and 3.31-4.32 GHz in measurements for state 2. Meanwhile, the antenna operating bandwidth in state 3 is 4.86-5.87 GHz in simulation and 4.98-5.96 GHz in measurements. In simulations and measurements, the antenna in state 4 covered the operating bands 3.38-5.96 and 3.31-6.03 GHz, respectively. Across all operational bands, the proposed antenna exhibits excellent impedance matching. The simulated and observed values varied marginally due to diode mapping, prototyping tolerance levels, and connection losses.

B. Far field analysis

The far-field analysis is crucial and investigated for evaluating the proposed antenna performance using an electromagnetic simulator and anechoic chamber. Figure 12 depicts the prototyped antenna radiation pattern in all states. In the yz-plane, the antenna produces omni-directional patterns, while in the xz-plane, it produces bi-directional patterns. Figures 12 (a)-(b) shows the antenna pattern in state 1 at 4.3 GHz, which has a simulated gain of 2.1 dB but a measured gain of 1.91 dB. Figures 12 (c)-(d) depict the measured radiation pattern in state 2 at 3.7 GHz.

In the simulation, the antenna has a gain of 2.3 dB, while in measurements, it has a gain of 1.86 dB. Similarly, in states 3 and 4, the pattern in Figs. 12 (e)-(h) is obtained at 5.5 and 3.7 GHz. The simulated and observed gains are 2.2/2.0 and 2.3/2.0 dB, respectively. In the simulation, the antenna has radiation efficiencies of 87.1, 86.4, 88.9, and 92.1 percent, and in measurements, it has radiation efficiencies of 80, 78, 83, and 86 percent. The antenna cross-polarization is < -15 dB in all states. Table 3 presents the simulated and observed values of the presented antenna in all four operating states.

Table 3: Operating states and performance

States	Freq. Bands (GHz) Simulated/Measured	Antenna Gain (dB) Simulated/Measured	Antenna Radiation Efficiency (%) Simulated/Measured
1	3.85-5.32 / 3.78-4.98	2.1 / 1.91	87.1 / 80
2	3.38-4.24 / 3.31-4.32	2.3 / 1.86	86.4 / 78
3	4.86-5.87 / 4.98-5.96	2.2 / 2.0	88.9 / 83
4	3.38-5.96 / 3.31-6.03	2.3 / 2.0	92.1 / 86

Table 4: Performance comparison with other works

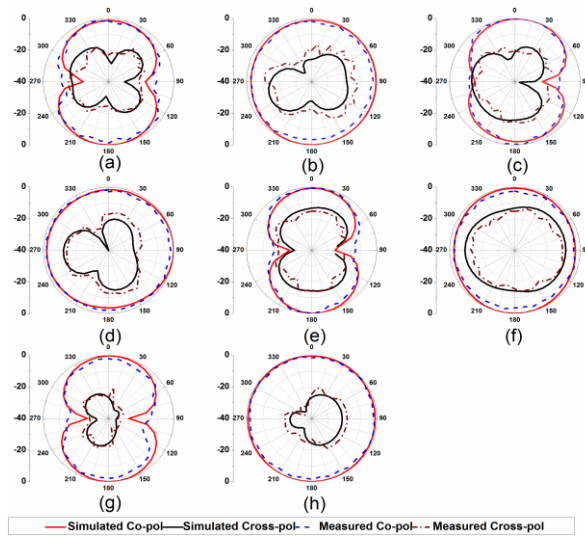| Ref.	Size (mm^2)	Sensing Band (GHz)	Communicating Band (GHz)	Is same Antenna have both Sensing and Communication Capabilities?	Radiation Efficiency (%)
[9]	50×46	-	2.2-4.75(Six Bands)	No	-
[15]	70×70	2-6	2.4, 2.75, 4.2	No	>70
[19]	68×51	2.63-3.7	2.63-3.7	Yes	-
[21]	60×50	2-5.7	3.21-4.0	Yes	>75
[22]	37.5×37.5	2.3-4.5	3.15-4.15, 2.65-3.85	Yes	>70
[23]	27×56	1-4.5	0.9-2.6(continuous)	Yes	> 70
This work	25×25	3.31-6.03	3.78-4.98, 3.31-4.32 4.98-5.96	Yes	>78

Fig. 12. Normalized gain pattern. State 1 (a) E-plane at 4.3 GHz; (b) H-plane at 4.3 GHz; State 2 (c) E-plane at 3.7 GHz; (d) H-plane at 3.7 GHz; State3 (e) E-plane at 5.5 GHz; (f) H-plane at 5.5 GHz; State 4 (g) E-plane at 3.7 GHz; (h) H-plane at 3.7 GHz.

IV. COMPARISON OF PERFORMANCE WITH PREVIOUS WORKS

Table 4 compares the proposed antenna to other antenna designs for similar applications that have been published. In contrast to the designs in [9,15,19,21,22, and 23], the proposed design is more compact. In addition, the antenna has radiation efficiency over 78 percent in all operating bands. Finally, this design operates in the sub-6 GHz band, covering almost the entire lower band (3.1-3.85 GHz), nR77 (3.3-4.2 GHz), and nR79 (4.4-5.0 GHz) in the 5G spectrum, as well as the entire higher band (4.8-6.0 GHz). In addition, the proposed antenna supports a variety of wireless communication systems, including WiMAX (3.3-3.8, 5.15-5.85 GHz), WLAN (5.1-5.3 GHz), and UWB (3.0-6.0 GHz).

V. CONCLUSION

This article demonstrated a quad-band frequency tunable antenna for 5G sub-6GHz applications. A slotted ground structure and a reconfigurable matching stub loaded to the feed line were used to achieve frequency reconfigurability with a consistent radiation pattern. Three PIN diodes were used to electronically tune the antenna. The antenna covered 3.31-6.03 GHz in sensing mode, and three bands in communication mode: 3.31-4.32, 3.78-4.98, and 4.98-5.96 GHz. The designed antenna has compact size, measuring 25×25×1 mm^3. The antenna has an excellent cross polar level, gain, and efficiency. The prototyped antenna is capable of detecting and communicating in the sub-6 GHz band. As a result, the design shown here could be used in cognitive radio and future communication systems.

ACKNOWLEDGMENT

REFERENCES

[1] Spectrum for 4G and 5G, *Qualcomm Technol. Inc.*, San Diego, CA, USA, Dec. 2017.

[2] IEEE: IEEE 5G and Beyond Technology Roadmap White Paper, October, 2017.

[3] International Telecommunication Union, ITU-R: Technical feasibility of IMT in bands above 6 GHz, July 2015.

[4] X. Liu, X. Yang, and F. Kong, "A frequency-reconfigurable monopole antenna with switchable stubbed ground structure," *Radio Engineering*, vol. 24, pp. 449-454, 2015.

[5] A. Gupta and R. K. Jha, "A survey of 5G network: Architecture and emerging technologies," *IEEE Access*, vol. 3, pp. 1206-1232, 2015.

[6] P. Gardner, M. R. Hamid, P. S. Hall, J. Kelly, F. Ghanem, and E. Ebrahimi, "Reconfigurable antennas for cognitive radio: Requirements and potential design approaches," *Institution of Engineering and Technology Seminar on Wideband, Multiband Antennas and Arrays for Defense or Civil Applications*, pp. 89-94, Mar. 2008.

[7] L. Ge and K. Luk, "Frequency-reconfigurable low-profile circular monopolar patch antenna," *IEEE Trans. Antennas Propag.*, vol. 62, no. 7, pp. 3443-3449,2014.

[8] G. Chen, X. Yang, and Y. Wang, "Dual-band frequency-reconfigurable folded slot antenna for wireless communications," *IEEE Antennas Wirel. Propagation Lett.*, vol. 11, pp. 1386-1389, 2012.

[9] H. A. Majid, M. K. A. Rahim, M. R. Hamid, and M. F. Ismail, "A compact frequency-reconfigurable narrowband microstrip slot antenna," *IEEE Antennas Wirel. Propag. Lett.*, vol. 11, pp. 616-619, 2012.

[10] V. Rajeshkumar and S. Raghavan, "A compact frequency reconfigurable split ring monopole antenna for WLAN/WAVE applications," *Applied Computational Electromagnetics Society Journal*, vol. 30, no. 3, pp. 338-344, 2015.

[11] S. Chilukuri, K. Dahal, A. Lokam, and W. Chen "A CPW fed T-shaped frequency reconfigurable antenna for multi radio applications," *Applied Computational Electromagnetics Society Journal*, vol. 33, pp. 1276-1285, 2018.

[12] H. Rajagopalan, J. M. Kovitz, and Y. Rahmat-Samii, "MEMS reconfigurable optimized E-shaped patch antenna design for cognitive radio," *IEEE Trans. Antennas Propag.*, vol. 62, no. 3, pp. 1056-1064, 2014.

[13] E. Erfani, J. Nourinia, C. Ghobadi, M. Niroo-Jazi, and T. A. Denidni, "Design and implementation of an integrated UWB/Reconfigurable-slot antenna for cognitive radio applications," *IEEE Antennas Wirel. Propag. Lett.*, vol. 11, pp. 77-80, 2011.

[14] Y. Tawk and C. G. Christodoulou, "A new reconfigurable antenna design for cognitive radio," *IEEE Antennas Wirel. Propag. Lett.*, vol. 8, pp. 1378-1381, 2009.

[15] J. Costantine, Y. Tawk, J. Woodland, N. Flaum, and C. Christodoulou, "Reconfigurable antenna system with a movable ground plane for cognitive radio," *Microw. Antennas Propag. IET*, vol. 8, pp. 858-863, 2013.

[16] S. S. Tripathi and C. C, "A novel reconfigurable antenna with separate sensing mechanism for CR system," *Prog. Electromagn. Res. C*, vol. 72, pp. 187-196, 2017.

[17] A. Nella and A. S. Gandhi, "A five-port integrated UWB and narrowband antennas system design for CR applications," *IEEE Trans. Antennas Propag.*, vol. 66, no. 4, pp. 1669-1676, 2018.

[18] H. Boudaghi, M. Azarmanesh, and M. Mehranpour, "A frequency-reconfigurable monopole antenna using switchable slotted ground structure," *IEEE Antennas Wirel. Propag. Lett.*, vol. 11, pp. 655-658, 2012.

[19] A. Mansoul, F. Ghanem, M. R. Hamid, and M. Trabelsi, "A selective frequency-reconfigurable antenna for cognitive radio applications," *IEEE Antennas Wirel. Propag. Lett.*, vol. 13, pp. 515-518, 2014.

[20] G. Srivastava, A. Mohan, and A. Chakrabarty, "A compact reconfigurable UWB slot antenna for cognitive radio applications," *IEEE Antennas Wirel. Propag. Lett.*, vol. 16, pp. 1139-1142, 2016.

[21] S. R. Thummaluru, M. Ameen, and R. K. Chaudhary, "Four-port MIMO cognitive radio system for midband 5G applications," *IEEE Trans. Antennas Propag.*, vol .67, no. 8, pp. 5634-5645, 2019.

[22] T. Alam, S. R. Thummaluru, and R. K. Chaudhary, "Integration of MIMO and cognitive radio for sub-6 GHz 5G applications," *IEEE Antennas Wirel. Propag. Lett.*, vol. 18, no. 10, pp. 2021-2025, 2019.

[23] X. Zhao, S. Riaz, and S. Geng, "A reconfigurable MIMO/UWB MIMO antenna for cognitive radio applications," *IEEE Access*, vol. 7, pp. 46739-46747, 2019.

[24] K. G. Thomas and M. Sreenivasan, "A simple ultrawideband planar rectangular printed antenna with band dispensation," *IEEE Trans. Antennas Propag.*, vol. 58, no. 1, pp. 27-34, 2009.

[25] K. P. Ray, "Design aspects of printed monopole antennas for ultra-wide band applications," *International Journal of Antennas and Propagation*, vol. 2008, 8 pages, 2008.

[26] D. Kapoor, V. Sangwan, C. M. Tan, V. Paliwal, and N. Tanwar, "Optimization of a T-shaped MIMO antenna for reduction of EMI," *Applied Sciences*, vol. 10, no. 9, p. 3117, 2020.

E. Sivakumar received his M.Tech in Applied Electronics in 2006 from Dr M.G.R Educational Research Institute of Science and Technology. He is pursuing Ph.D. in SRM Institute of Science and Technology, India. His research interest includes antenna design, reconfigurable antennas, RF and microwave circuit design.

B. Ramachandran received his bachelor's degree in Electronics and Communication Engineering from Thiagarajar College of Engineering, Madurai, in 1990 and master's degree in Satellite Communications from National Institute of Technology, Trichy, in 1992. He obtained his Ph.D. degree in the area of Wireless Mobile Networks from Anna University, Chennai, in 2009. At present, he is working as Professor at SRM University in Chennai. He authored a textbook on digital signal processing. His teaching and research interests include digital communication, wireless networks, UWB antenna design, network security, and mobile computing. He has published 37 research papers in national and international conferences and journals. He was awarded IETE-SK Mitra Memorial Best Research Paper Award in 2009. He is a member of ISTE, and fellow of IE(I) and IETE.